

# Synthesis, growth, and characterizations of bis-ethylene diammonium diphenolsulfonate monohydrate single crystal: Optoelectronic and antibacterial aspects

N. Rama Krishna Chand<sup>a</sup>, Y. Subba Reddy<sup>b</sup>, J. Theodore<sup>c</sup>, M. Antilin Princela<sup>d</sup>, S. Suguna<sup>e,\*</sup>, P. Lakshmi Praveen<sup>f,\*</sup>

<sup>a</sup> Department of Physics, Andhra Loyola College (Autonomous), Vijayawada 522008, India

<sup>b</sup> Department of Chemistry, Andhra Loyola College (Autonomous), Vijayawada 522008, India

<sup>c</sup> PG and Research Department of Physics, Queen Mary's College, Chennai 4, India

<sup>d</sup> Department of Chemistry, Holy Cross College (Autonomous), Nagercoil-629004, Tamil Nadu, India

<sup>e</sup> PG Department of Chemistry, Shrimathi Devkunvar Nanalal Bhatt Vaishnav College for Women (Autonomous), Chennai 44, India

<sup>f</sup> Department of Physics, Veer Surendra Sai University of Technology, Burla 768018, Sambalpur, Odisha, India

## ARTICLE INFO

### Keywords:

Organic compound  
Crystal growth and structure  
Photoluminescence  
Second harmonic generation  
Antibacterial studies

## ABSTRACT

Bis-Ethylene Diammonium di-Phenolsulfonate monohydrate (EDDSM) single crystal was amalgamated by the process of slow evaporation solution with water and ethanol as blended solvents at room temperature. The synthesized crystal EDDSM structure was resolved by diffraction of X-rays using single crystal technique. The identification of different functional groups, various kinds of carbon atoms as well as protons in the EDDSM crystal were established by <sup>13</sup>C and <sup>1</sup>H NMR spectra respectively. The optical properties were studied, using optical absorption along with photoluminescence studies. The stability of EDDSM single crystal against temperature and mechanical stress was studied by examining TGA/DTA and Vickers micro hardness respectively. The nonlinear nature of the grown EDDSM was observed and established by 'Second Harmonic Generation' (SHG). The antibacterial and antifungal activities of EDDSM was evaluated using *Staphylococcus aureus*, *Streptococcus mutans*, *Klebsiella pneumoniae*, *Pseudomonas aeruginosa* whereas *Aspergillus niger* and *Candida albicans*. These reported features and characterizations establish the reported compound as a promising crystal.

## 1. Introduction

Owing to its superiority over conventional inorganic materials, organic crystals have a wide range of possible uses that have attained curiosity for several years. The potentialities of organic materials are their comparatively higher electronic sensitivity due to molecules polarizability, their superficial customization using paradigmatic artificial procedures, and their relative ease of device distribution [1]. Due to their conjugated (delocalized)  $\pi$ -electron clouds connecting the acceptor (A), and electron donor (D) as well as their asymmetric charge transfer character, organic materials produces macroscopic nonlinearities [2–5]. Further benefits include synthetic flexibility through molecular engineering and chemical synthesis for device applications like optical computing, switching, power limitation, double-photon based scanning laser microscopy, and optical switching [6,7].

Conversely, significant NLO responses across a broad range of frequency, low dielectric constants, ultrafast response times, and larger laser damage thresholds are observed in organic non-linear crystals [8]. Furthermore, because they have potential uses in nonlinear optics and drug administration, organic crystals are important in the fields of supramolecular chemistry, biological sciences, and crystal engineering etc. [9,10].

Generally speaking, among the organic acceptor compounds disclosed in NLO applications, a number of organic charges transfer crystals of p-toluenesulfonic acid. These crystal materials consist of chemically pure  $\pi$ -conjugated molecules, which give rise to a model for ordered superior structures [11,12]. Amide and acid are two of the more interesting pairings to investigate the fundamental electrical characteristics of organic semiconductor materials. They generate a non-centrosymmetric crystal structure with good NLO performance [13,

\* Corresponding authors.

E-mail addresses: [sugunaganga08@gmail.com](mailto:sugunaganga08@gmail.com) (S. Suguna), [plpraveen\\_phy@vssut.ac.in](mailto:plpraveen_phy@vssut.ac.in) (P.L. Praveen).

<https://doi.org/10.1016/j.molstruc.2024.137926>

Received 31 December 2023; Received in revised form 10 February 2024; Accepted 1 March 2024

Available online 1 March 2024

0022-2860/© 2024 Elsevier B.V. All rights reserved.

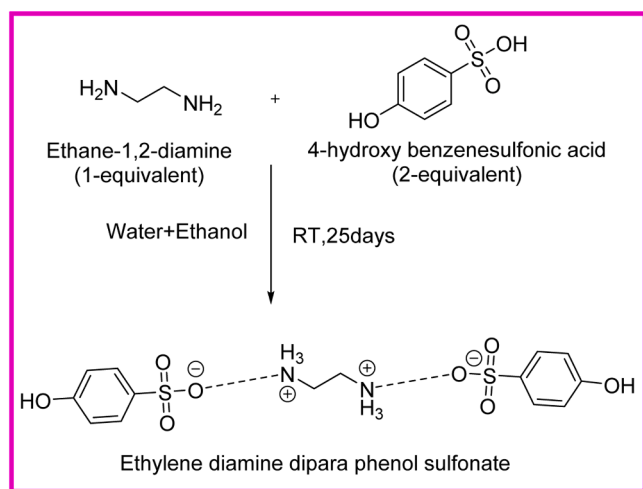


Fig. 1. Preparation of EDDSM salt.

14].

One of the rapidly expanding multidisciplinary fields is the creation of multi functionalized compounds with desirable physicochemical characteristics for practical applications, such as ferroelectric, piezoelectric, ferromagnetic, and NLO properties [15,16]. Due to the existence of a delocalized electronic  $\pi-\pi^*$  architecture between the donor and acceptor ( $D < \pi > A$ ), that increases the material's non-linear optical properties by causing non-linear optical susceptibility, and asymmetric polarizability, these organic crystals offer a huge and swift non-linear activity for optical excitation, large electro-optic coefficient (EO), high optical damage threshold, small dielectric constant, greater optical susceptibility, and natural synthetic flexibility [17,18]. In spite of dominant mechanical, chemical, and thermal stabilities, numerous inorganic crystals suffer from less qualitative NLO properties [19].

The ethylene diamine ( $-NCH_2CH_2N-$ ) exhibits well-documented biological activities. The ethylene diamine derivatives illustrate cytotoxic action, that causes not only arrest of cells at diverse stages of cell cycle but also loss in potential of mitochondrial membrane in these cancer cells which are useful in developing future drugs. Substances with ethylene diamine ( $-NCH_2CH_2N-$ ) show activities such as antimicrobial, -fungal, -bacterial, -tuberculosis and -cancer. They are also used in Ligation of water to magnesium chelates which are of biological importance. These derivatives find their uses in finding out, the effect of aging of thin films made up of plasma ethylenediamine (PPEDA) polymerized with plasma on cell-adhesive implant coatings. They are also used in exploring novel modified vitamin B<sub>12</sub> as a drug carrier which is being probed for future pharmaceutical uses [20,21]. Ethylenediamine derivatives are also useful as materials that provide enviable solubility, sustained release in addition to boost up absorption to drugs or else nutraceuticals [2–5]. The HSO<sub>3</sub> group present in phenol sulfonic acid donates proton and involves in bond formation as a sulfonate group ( $-SO_3^-$ ). The non-centro symmetric crystals such as *N*-(4-[Dimethyl amino] benzylidene)-4-methylaniline and 4-methyl anilinium *p*-toluene sulfonate moreover the potential applications of single crystals along with their amalgamation, bulk growth as well as characteristic studies of 4-methyl anilinium phenol sulfonate were mentioned in earlier literature [6–10]. The current exploration as regards amalgamation, bulk growth as well as characteristic properties like structural, spectral, optical, mechanical as well as thermal for grown crystal Bis-Ethylene diammonium di-phenol sulfonate monohydrate (EDDSM) were carried out and the end results are disclosed. The synthesized organic single crystal EDDSM has wide applications in industry and pharmacy.

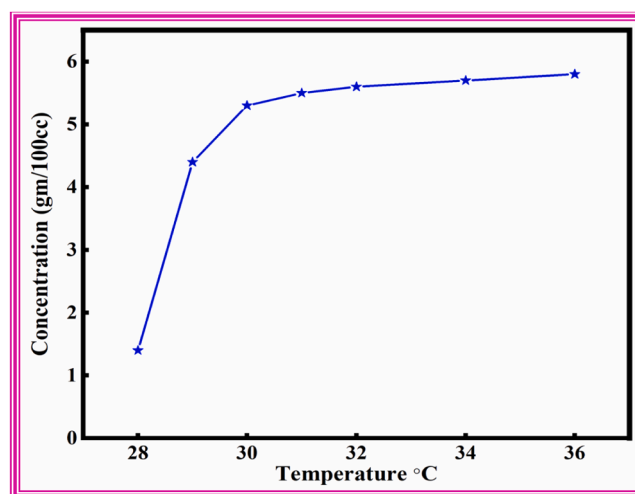


Fig. 2. Variation of solubility of EDDSM in the solution of ethanol and water with respect to temperature.

## 2. Experimental methods

### 2.1. Amalgamation of EDDSM

Green solvents such as H<sub>2</sub>O and EtOH were gaining the importance in the synthetic organic chemistry and accordingly this methodology was planned [22,23]. The current EDDSM crystal was amalgamated by the chemical reaction of ethylene diamine (Loba) with phenolsulfonic acid (Aldrich) in the molar ratio 1:2. In the first step of the procedure, Phenolsulfonic acid (3.4 g) was dissolved in water (10 ml) and added slowly to a predissolved solution of Ethylene diamine (6 ml) in EtOH (15 ml) at room temperature. Secondly, this homogeneous mixture was stirred for 6 hrs and is allowed to crystallize (Ethylene diammonium diphenolsulphonic acid) for a period of 21 days through slow evaporation after filtration at room temperature as represented in Fig. 1 below.

### 2.2. Growth of EDDSM crystal and solubility study

The EDDSM crystal was harvested at 25th day and checked its solubility for nucleation preparation of bulky crystal growth. A small quantity of synthesized salt was made use of in solubility analysis using various organic solvents such as ethanol, methanol, acetone, Acetonitrile and chloroform. Solubility analysis clearly indicates that EDDSM salt is very much soluble in the combined solution of ethanol as well as water taken in equal quantities and hence motivated to choose their combination as an appropriate suitable solution for the crystal growth. The prominent factors that influence the growth of a single large crystal of good quality are temperature as well as its solubility in a solvent [24]. The experimental study on solubility of current EDDSM crystal was done in the mixture of ethanol and water as blended solvent stirring with immersible stirrer, subjected to a temperature range of 28–36 °C by using a constant temperature bath by means of cryostat capability up to an accuracy of  $\pm 0.01$  K. The weight loss of solute was noted down and variation of solubility EDDSM against temperature is represented in the Fig. 2. This analysis on solubility of EDDSM single crystals indicates clearly that mixture of ethanol and water in equal magnitude would be appropriate solvent along with slow evaporation method is suitable for growth of single large EDDSM crystals at room temperature.

Equal amounts of ethanol and water taken in a solution was used as a solvent to prepare saturated EDDSM solution which was maintained steady at 28 °C temperature by keeping in an invariable temperature bath in addition to keep away from the consequence of ebb and flow in room temperature. After performing the process of slow evaporation for a duration of one month, crystals grown were harvested with dimensions



Fig. 3. Synthesized EDDSM crystal.

nearly  $2.0 \times 1.5 \times 0.3 \text{ cm}^3$  furthermore to have advance studies recrystallization was allowed to nurture pure crystals. Fig. 3 represents single large EDDSM crystal.

### 3. Characterization studies

Bruker X-ray diffractometer of model AXS (Kappa Apex II) was used to obtain X-ray diffraction data of the synthesized EDDSM crystal by means of  $K_{\alpha}$  radiation of molybdenum having  $0.712 \text{ \AA}$  wavelength at room temperature. The atom numbering scheme was involved to have nearly 30 % probability thermal displacement ellipsoids for the ORTEP view of compound [25]. The structure of synthesized EDDSM studied by involving 'SHELXS-97' either by direct method or full matrix least squares with R value in the range of 0.030 to 0.087 [26].

JASCO FTIR 410 spectrometer was used to record FTIR spectrum of synthesized EDDSM single crystal based on the method of KBr pellet. The structure of EDDSM grown was done by Bruker (Ultra shield) 300 MHz TM instrument with DMSO solvent was used to record  $^1\text{H}$  NMR operating with a frequency of 300 MHz whereas 75 MHz frequency was used to record  $^{13}\text{C}$  NMR spectrum of EDDSM at  $23 \text{ }^{\circ}\text{C}$ . The optical absorption of the synthesized sample obtained with Perkin-Elmer Lambda 35 spectrometer with EDDSM of 1 mm in thickness from 200 nm to 1100 nm. Argon ion ultra violet laser having wavelength of 244 nm was made use of in exciting the electrons present in synthesized crystal to study the photoluminescence. For analyzing the luminescence of EDDSM crystal, Horiba Jobin monochromatic 330 nm and 550 nm PMT detectors were used. The PerkinElmer Diamond TG/DTA instrument has been utilized for recording the TG/DTA of EDDSM single crystal for which a platinum crucible has been made use of, for heating the sample in nitrogen atmosphere by heating especially from  $23 \text{ }^{\circ}\text{C}$  to  $275 \text{ }^{\circ}\text{C}$  with frequency  $10 \text{ }^{\circ}\text{C}/\text{min}$ . MATSUZAWA model MMT-Xseries micro hardness tester provided with indenter made of diamond used on behalf of measuring Vickers micro-hardness of EDDSM crystal. The stock solution was prepared by dissolving  $100 \text{ }\mu\text{g}$  of EDDSM in 1 ml of DMSO,  $5 \text{ }\mu\text{l}$  ( $50 \text{ }\mu\text{g}/\text{disc}$ ) of EDDSM extract was added into the Sterile Whatman filter paper (diameter 6 mm) and permitted to dry at room temperature which was further incubated for 24 h at  $37 \text{ }^{\circ}\text{C}$ . The antibacterial activity of the synthesized amalgam was known by studying disc diffusion process on inhibition zone where as antifungal activities of present sample were analyzed on dextrose agar plates by incubating over duration of 48 to 72 h at  $27 \text{ }^{\circ}\text{C}$ . Streptomycin in addition to Amphotericin B were used as standard to record inhibition zone thickness produced in opposition to bacteria and fungus which demonstrates that EDDSM possesses good antibacterial and antifungal activity against *Staphylococcus aureus*, *Streptococcus mutans*, *Klebsiella pneumoniae*, *Pseudomonas aeruginosa*

Table 1

Structural data along with elegance for EDDSM.

Empirical formula	$\text{C}_{16} \text{H}_{20} \text{N}_2 \text{O}_{10} \text{S}_2$
Molecular weight	464.46
Temperature	293 K
Wavelength	$0.71073 \text{ \AA}$
Crystal system, space group	Triclinic, $P\bar{1}$
Unit cell dimensions	$a = 5.5218(4) \text{ \AA}$ $b = 7.2785(6) \text{ \AA}$ $c = 23.6082(19) \text{ \AA}$ $\alpha = 97.787(4) \text{ deg.}$ $\beta = 92.157(4) \text{ deg.}$ $\gamma = 91.852(4) \text{ deg.}$
Volume	$938.74(13) \text{ \AA}^3$
Calculated density, Z	$2, 1.643 \text{ Mg/m}^3$
Absorption coefficient	$0.346 \text{ mm}^{-1}$
F(000)	484
Size of crystal	$2.3 \times 2.5 \times 1 \text{ mm}$
Range of theta to collect data	$0.87 \text{ to } 26.55 \text{ deg.}$
Limiting indices	$-6 < h < 6, -9 < k < 9, -29 < l < 29$
Reflections collected / unique	$11,837 / 6485$ [R(int) = 0.0360]
Completeness to theta	$=26.55^\circ$ 95.9 %
Refinement methodology	Full-matrix least-squares on $F^2$
Data / restraints / parameters	$6485 / 11 / 541$
Goodness-of-fit on $F^2$	1.296
Final R indices [ $I > 2 \text{ sigma}(I)$ ]	$R1 = 0.0942, wR2 = 0.3194$
R indices (all data)	$R1 = 0.1030, wR2 = 0.3258$
Absolute structure parameter	$0.4(3)$
Largest diff. peak and hole	$1.423 \text{ and } -0.980 \text{ \AA}^{-3}$

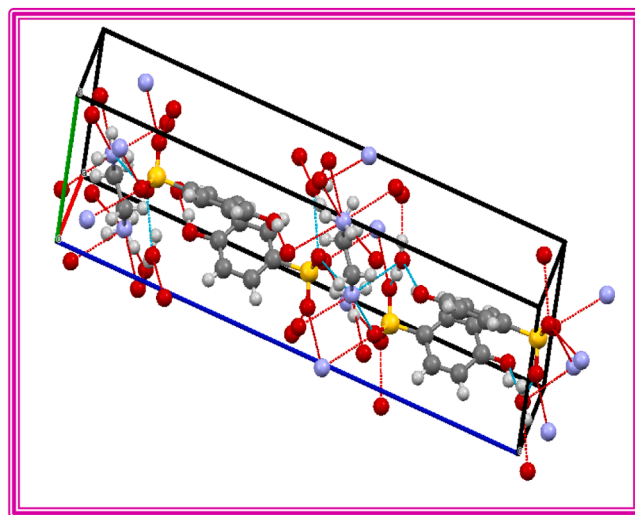


Fig. 4. The molecular packing viewed along 'b' axis.

whereas *Aspergillus niger* and *Candida albicans* respectively.

## 4. Results and discussion

### 4.1. Studies on X-ray diffraction

The information collected in X-Ray diffraction of EDDSM single crystal, 6485 out of 11,837 reflections noted within the range  $0.87^\circ$ – $26.55^\circ$  possess unique reflections. EDDSM crystal have Centro symmetric space group  $P\bar{1}$  more over the EDDSM crystallizes into centric triclinic as indicated by the systematic absence of (h, k, l). The dimensions of unit cell of EDDSM crystal is given by  $a = 5.5218(4) \text{ \AA}$ ,  $b = 7.2785(6) \text{ \AA}$ ,  $c = 23.6082(19) \text{ \AA}$ ,  $\alpha = 97.7887(4)^\circ$ ,  $\beta = 92.157(4)^\circ$ ,  $\gamma = 91.852(4)^\circ$ , volume =  $938.74 \text{ \AA}^3$ . The Table 1 indicates crystallographic structural data of EDDSM crystal whereas Fig. 5 represents the label design of ORTEP diagram of EDDSM crystal having a probability of 30 %. The ordered molecular packing is shown and demonstrated in the

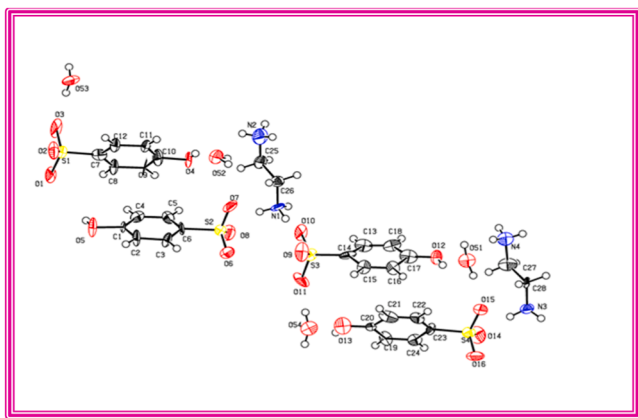


Fig. 5. The labeling design for ORTEP diagram of EDDSM crystal comprising 30 % probability.

Table 2  
Selected Bond lengths and angles [ $\text{\AA}$  and  $^\circ$ ] for EDDSM.

Bonds	Bond lengths [ $\text{\AA}$ ]
C(1)–C(2)	1.380(2)
C(1)–C(6)	1.386(2)
C(1)–S(1)	1.7662(16)
C(2)–C(3)	1.380(2)
C(3)–C(4)	1.382(2)
C(4)–O(4)	1.3603(19)
C(4)–C(5)	1.385(2)
C(5)–C(6)	1.375(2)
C(7)–C(12)	1.385(3)
C(7)–C(8)	1.387(2)
C(7)–C(13)	1.501(3)
C(8)–C(9)	1.374(3)
C(9)–C(10)	1.376(2)
C(10)–C(11)	1.374(2)
O(1)–S(1)	1.4487(12)
O(2)–S(1)	1.4414(13)
O(3)–S(1)	1.4556(13)
Bonds	Angles [ $^\circ$ ]
C(2)–C(1)–C(6)	119.85(15)
C(2)–C(1)–S(1)	120.82(12)
C(6)–C(1)–S(1)	119.30(12)
C(1)–C(2)–C(3)	119.81(15)
C(2)–C(3)–C(4)	120.32(15)
O(4)–C(4)–C(3)	117.48(14)
O(4)–C(4)–C(5)	122.66(14)
C(3)–C(4)–C(5)	119.85(15)
C(6)–C(5)–C(4)	119.78(15)
C(5)–C(6)–C(1)	120.38(14)
C(12)–C(7)–C(13)	120.91(17)
C(8)–C(7)–C(13)	121.46(17)
C(9)–C(8)–C(7)	121.47(17)
C(10)–C(11)–C(12)	118.74(16)
C(11)–C(12)–C(7)	121.83(16)
O(2)–S(1)–O(1)	112.76(8)
O(2)–S(1)–O(3)	113.86(8)
O(1)–S(1)–O(3)	110.38(8)
O(2)–S(1)–C(1)	106.67(7)
O(1)–S(1)–C(1)	106.46(7)
O(3)–S(1)–C(1)	106.13(7)

(010) direction in Fig. 4.

In either inter or intra molecular hydrogen bonding generally hydrogen atom bounded with one electronegative atom like nitrogen and interacts with another electronegative atom by means of electrostatic forces. In present situation 'a' axis view was used for orderly arrangement of EDDSM molecule. The bond angles as well as bond lengths of the crystal synthesized tabulated in Table 2 and these reported values are in accordance with that of phenyl ring and functional groups

Table 3

Bond lengths ( $\text{\AA}$ ) in addition to bond angles (in degrees) made by hydrogen atoms of EDDSM.

JLVD-H...A	d(D-H)	d(H...A)	d(D...A)	<(DHA)
N(1)-H(1A)...O(2)#	0.89	1.94	2.809(2)	165
1 N(1)-H(1B)...O(4)#2	0.89	1.96	2.839(2)	169
N(1)-H(1C)...O(1)#3	0.89	1.96	2.836(2)	169
N(1)-H(1C)...S(1)#3	0.89	2.80	3.551(2)	142
O(4)-H(4)...O(3)#1	0.82	1.82	2.634(2)	172
O(4)-H(4)...S(1)#1	0.82	3.01	3.778(2)	157

Symmetry transformations used to generate equivalent atoms:

#1x, -y + 1/2, z - 1/2 #2 -x + 1, -y, -z #3x, -y - 1/2, z - 1/2.

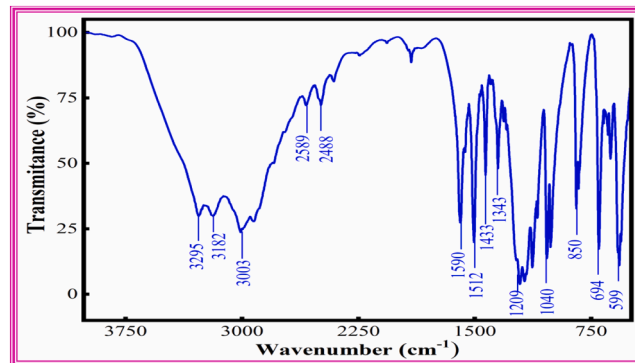


Fig. 6. FTIR spectrum of synthesized EDDSM crystal.

attached with it [27,24]. The length of C–C bonds present in phenyl rings is within the range 1.375(2)  $\text{\AA}$ –1.386(2)  $\text{\AA}$  where as other C–C bond lengths lie in between 1.376(2)  $\text{\AA}$  and 1.387(2)  $\text{\AA}$ . The earlier literature documented values correlate with present bond lengths of C–C as well as N–C occurring in EDDSM crystal but the bond length of C1–S1 is to some extent fewer than the regular value [20–22]. The range in bond angles of phenyl units present in the present system is 118.8(2) $^\circ$ –121.8(3) $^\circ$ . The groups present in the crystal such as NH<sub>3</sub>, SO<sub>3</sub> as well as CH<sub>3</sub> give a deviation from 120 $^\circ$ . It is a well known fact that the double bond causes slightly larger angles [28,29]. The exocyclic angles given by [C9/C10/N1] = 119.8(2) $^\circ$ , C10 [C11/C10/N1] = 119.2(2) $^\circ$ , and around S1 [O1/S1/C1] = 106.48(1) $^\circ$ , [O3/S1/C1] = 106.13 $^\circ$  and [O2/S1/C1] = 106.67(1) $^\circ$  respectively clearly indicates that amine and sulphur groups are in coplanar with that of respective benzene rings more over Sp<sup>2</sup> hybridization is present in the synthesized crystal as sum of all angles around N1 atom is [359.5(2) $^\circ$ ]. Intra-molecular hydrogen bonding especially C–H...O bonds stabilizes structure with dihedral angle of 51.6 (1)  $^\circ$  present in between the phenyl rings.

The crystal structure stabilization was done by N–H...O and O–H...O type of hydrogen bonds linking symmetrical molecules occurring at positions (x, y, z) (x, 1/2–y, –1/2 + z), giving rise to a dimer, R<sub>2</sub><sup>1</sup> by graph-set descriptor (2516). The molecular ribbon is formed by these dimers that run along 'bc' plane more over molecular sheets are formed due to linkage of adjacent molecular ribbons with hydrogen bonding through N–H...O bonds. The following Table 3 represents the bond lengths in addition to bond angles made by hydrogen atoms of EDDSM. The Cambridge Crystallographic Data Centre [CCDC No.1013776] provides crystallographic structural data of synthesized crystal EDDSM.

#### 4.2. Analysis of FTIR spectra

Infrared spectroscopy has been used extensively in the investigation of structure of crystal along with sonata of various organic and inorganic composites. Several workers in the field of crystal growth have been engaged in obtaining detailed structural information from IR

**Table 4**  
Spectral data assignments for EDDSM crystal.

Frequency (cm) <sup>-1</sup>	Assignments
3295	stretching vibrations of OH
3182	stretching vibrations of N <sup>+</sup> —H
3003	stretching vibrations of C—H
2589	CH <sub>2</sub> asymmetric vibration
2488	CH <sub>2</sub> symmetric vibration
1590	Asymmetrical stretching vibrations of C—C bonds
1512	Symmetrical stretching vibrations of C—C bonds
1433	Asymmetrical stretching vibrations of C—N bonds
1343	Symmetrical stretching vibrations of C—N bonds
1209	Asymmetrical stretching vibrations of SO <sub>3</sub> group
1040	Symmetrical stretching vibrations of SO <sub>3</sub> group
850	CH asymmetric bending vibrations
694	N—H out plane wagging
559	NH <sub>3</sub> <sup>+</sup> torsional oscillation

spectroscopy. Normally by making use of Infrared spectroscopy it is possible en route for discovering the functional groups in the current crystal under analysis. The intensity and position of the peaks can offer data about the categories of chemical bonds present in the compound under analysis. Generally, the peak position in an IR spectrum is connected to the frequency of the absorbed energy that is established by the explicit chemical bond under analysis. Fig. 6 indicate FTIR spectrum of EDDSM crystal within the wave number range 4000 cm<sup>-1</sup> to 500 cm<sup>-1</sup>. Accordingly, these groups occurring in present crystal absorb a particular frequencies based on their characteristic nature [14,15,27,30]. The strong hydrogen bonding present between phenol sulfonate and diethyl amine in the current EDDSM single crystal was mainly due to the

donation of H<sup>+</sup> from phenol sulfonic acid to amine group NH<sub>2</sub> group of diethyl amine that leads to formation of N<sup>+</sup>—H bond. The spectral data assignments for EDDSM are represented in Table 4 (Fig. 6).

#### 4.3. Analysis of NMR spectra

The existence of diverse variety of carbon atoms as well as protons in the EDDSM crystal were established by the <sup>13</sup>C and <sup>1</sup>H NMR spectra as represented in Fig. 7(a) and (b) respectively. The structure of any organic compounds can be analyzed by recording the above said analytical techniques [13,14,26,27]. The peak at δ 9.661 ppm in <sup>1</sup>H NMR spectrum of EDDSM crystal indicates protons in the water molecule where as the peak at δ 2.317 ppm and peaks appeared within the range δ 7.471–δ 7.443 ppm is by reason of the protons ortho as well as meta to hydroxyl group in the phenol moiety respectively. The NH<sub>3</sub><sup>+</sup> protons present in the amine group give peaks in between δ 6.726–δ 6.97 ppm. The peaks at δ 3.075 ppm and δ 3.444 ppm indicate the hydroxyl protons in the phenol moiety. The observed NMR spectrum peaks are studied to disclose the EDDSM crystal characteristics.

The chemical shift observed at δ 158.338 ppm and δ 138.827 ppm match up to the carbons attached to the hydroxyl group in the phenol moiety and sulfonate group respectively in the <sup>13</sup>C NMR spectrum of EDDSM crystal. The arised peaks at δ 127.588 ppm and δ 114.675 ppm represent carbons present in meta and para position to that of carbon attached to hydroxyl group respectively where as the peaks observed within the range δ 40.425 ppm–δ 39.423 ppm match up to carbons present in the ethylene group. Thus the molecular composite structure has been analyzed by <sup>1</sup>H and <sup>13</sup>C NMR spectra.

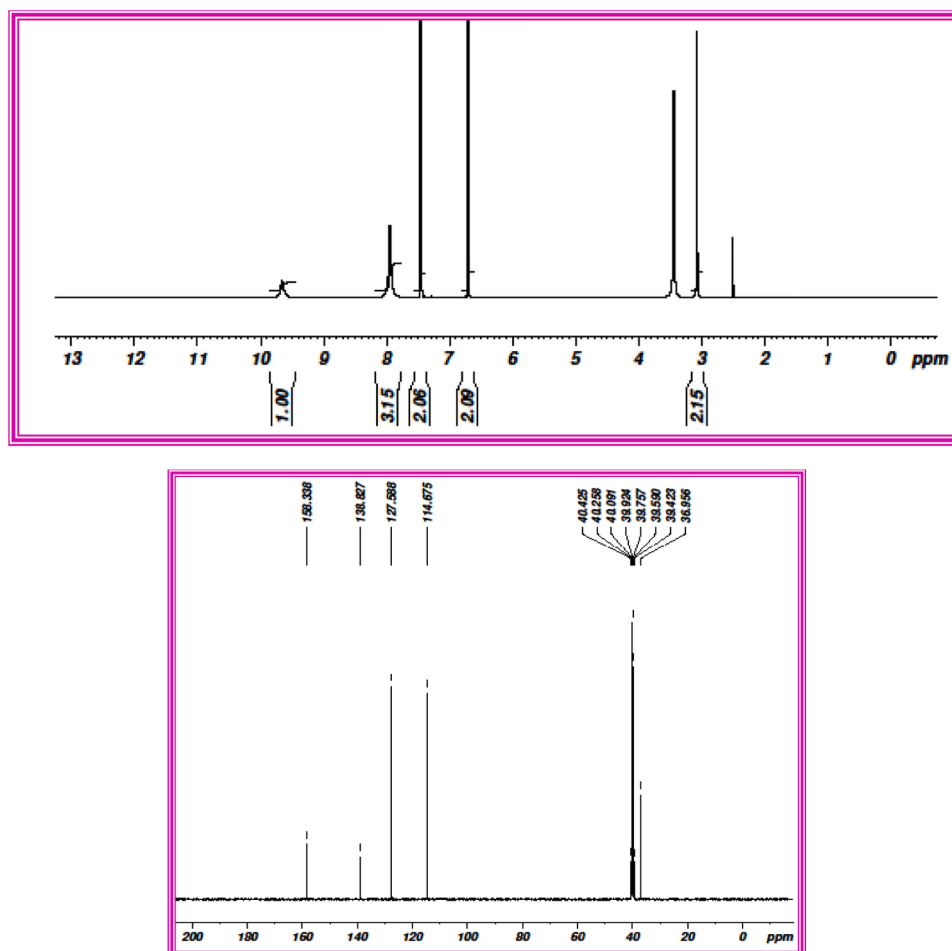


**Fig. 7.** (a) Representation of proton NMR spectrum of EDDSM crystal. (b) Representation of Carbon NMR spectrum of EDDSM crystal.

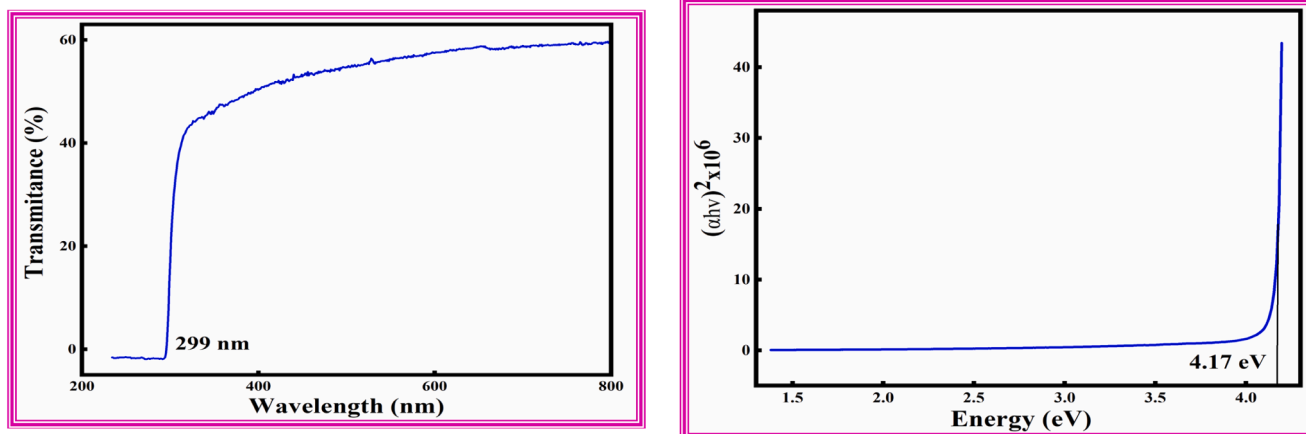


Fig. 8. (a). Optical absorption spectrum of EDDSM crystal. (b) Deviation of  $(\alpha h\nu)^2$  with  $h\nu$  in EDDSM crystal.

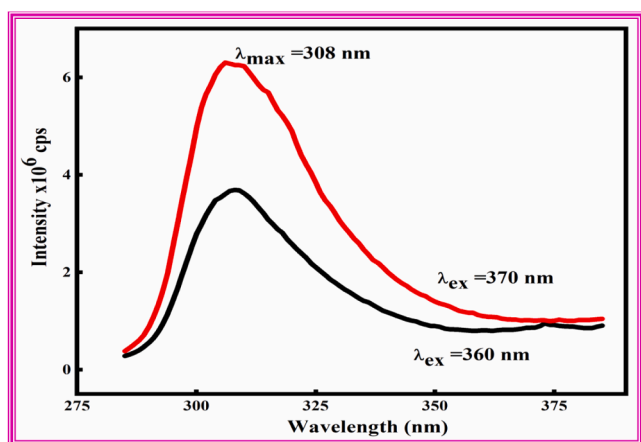


Fig. 9. Photoluminescence spectra of EDDSM crystal excited by wavelengths 360 nm and 370 nm.

#### 4.4. Analysis of optical absorption spectrum

Fig. 8(a) represents the optical absorption spectrum of EDDSM single crystal obtained within 200 to 800 nm range.

The ensuing transmission spectrum exemplifies that the grown crystal has a cut-off edge at 299 nm that reveals that the crystal is a good structure for frequency conversion applications. Further, one may infer from the figure that the transmittance of the grown crystal possesses almost 60 % in the visible region which is mainly owing to the  $\pi-\pi^*$  transition in the composite. The following relations were used to determine 'Optical energy band gap', ( $E_g$ ), 'absorption coefficient' ( $\alpha$ ) from the optical absorption spectrum of EDDSM crystal, of which transmittance ' $T$ ', crystal thickness ( $t$ ), optical band gap ( $E_g$ ), frequency ( $\nu$ ) of incident photons, Planck constant ( $h$ ), and  $A$  is a constant.

$$\alpha = \frac{2.3026 \left( \frac{1}{T} \right)}{t}$$

$$\alpha h\nu = A(E_g - h\nu)^{\frac{1}{2}}$$

The optical energy band gap of present EDDSM crystal was determined to be 4.17 eV. As indicated in Fig. 8(b). Thus EDDSM crystal possesses applications in the opto electronics owing to its large band gap [28]. The reported parameters are helpful to understand the UV stability of the compound as well as for UV filter, and sensor applications [31, 32].

#### 4.5. Studies on photoluminescence

Fig. 9 represents the spectrum of photoluminescence (PL) for EDDSM crystal obtained by using wavelengths of 260 nm and 270 nm for excitation at room temperature. It was clearly observed from the variation of intensity curve, that there is no change in position of emission peak with increase in excitation wavelength and induced polarization does not influence optical emission of EDDSM crystal.

The transitions from  $\pi-\pi^*$  taking place in the C=O groups of the present composite gives ultra violet emission peak at 270 nm with center at 4.02 eV on exciting with wavelength  $\lambda_{\max} = 308$  nm. The intermolecular interactions present within EDDSM crystal broaden the emission band and the crystalline character of synthesized EDDSM was confirmed by means of intensity and sharpness of the peaks observed in photoluminescence spectrum of EDDSM crystal. The increase in crystallinity behavior of EDDSM crystal was revealed by 'Full Width at Half Maximum', (FWHM) of peak emitted at 35.7 nm.

#### 4.6. Thermal study on EDDSM crystal

Differential thermogram analysis (DTA) as well as Thermo gravimetric analysis (TGA) made use of in studying thermal nature of synthesized EDDSM crystal subjected to a rise in temperature from 30 °C to 500 °C as represented by Fig. 9. TGA of the composite reveals that EDDSM crystal was observed to be stable up to 192 °C and on further increase in temperature there was a decrease in weight of the crystal as a result of decomposition more over the sharpness in the peaks indicate the crystalline nature of the composite [33,34]. The DTA of the EDDSM crystal gives endothermic peak at 210 °C and the peak sharpness represents the purity and crystalline nature of the present synthesized composite.

#### 4.7. Measurement of Vickers micro hardness

Micro hardness testing is a technique for determination of hardness of a material or resistance towards deformation when test compounds are not appropriate for macro-hardness. Micro hardness testing is perfect for the evaluation of hardness of very small/ thin samples, individual phases of a molecule, complex shapes, and surface coatings/platings. The mechanical properties of present synthesized EDDSM crystal has been carried out by measuring Vickers micro hardness on the smooth surface of crystal by varying loads from 1 g to 50 g having time for indentation preset to be 5 s used for applied loads at room temperature and the variation in micro hardness with the load applied is represented in Fig. 10. The following equation has been used to determine the hardness of EDDSM crystal

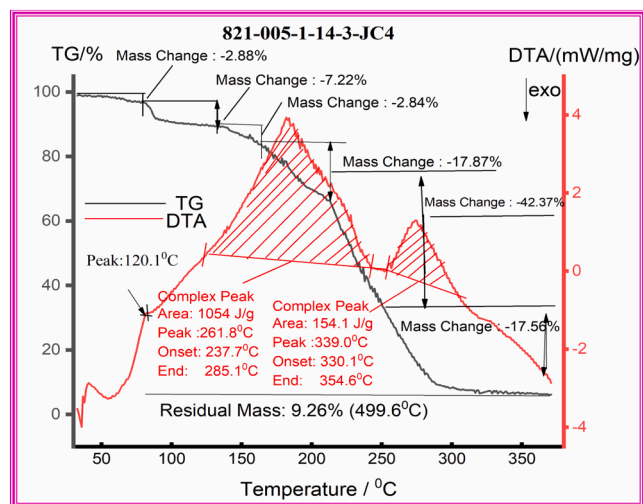


Fig. 10. TGA and DTA curves of synthesized EDDSM crystal.

$$H_v = \frac{1.8544P}{d^2} \text{ Kg/mm}^2$$

where ' $H_v$ ' is Vickers hardness number, ' $d$ ' is diagonal indentation length and ' $P$ ' is applied load. The mechanical studies reveal that there is an increase in hardness number up to an increase in load of 100 g there after wards as a result in the release of internal stress produced in the vicinity by means of indentation, several breaks were detected on the surface of EDDSM crystal [35].

#### 4.8. Measurement of efficiency in SHG

The Nd:YAG laser giving pulse at a frequency of 10 Hz in addition to wavelength of 1064 nm was made use of in measuring 'Second Harmonic Generation' (SHG) efficiency of grown EDDSM crystal by adopting modified technique proposed by Kurtz and Perry. The SHG presentation of the grown-up crystals is efficient for categorizing the materials with non-centrosymmetric (NCS) natural structures. The intermolecular strong interactions in semi-organic crystals results in a considerable wave functions overlap, which leads to the delocalization of  $\pi$ -electrons. The sample was firmly jam-packed in capillary tube of micro size after a through grinding and the relative efficiency in SHG of EDDSM was found by evaluating the outputs in SHG of a KDP sample with alike sized particles.

The comparative efficiency of EDDSM crystal with that of standard sample was observed to be 1.2. The SHG in the present synthesized crystal EDDSM was authenticated by a radiation of 532 nm, and efficiency level in SHG was determined by the amount of charge transfer (CT) over NLO chromophore on molecular scale. The grown crystal shows substantial evidence of NLO behavior although it belongs to Centro symmetric group. The efficiency of second harmonic generation of certain Centro symmetric crystals like 'glycinepicrate', 'diglycine picrate', 'R,S-Serine' and '2-methylimidazolium picrate' crystals were studied by Ghazaryan et al., Suguna et al., Dhanabal et al., Shakir et al., and Rieckoff and Peticoals [36–40]. In the present grown EDDSM crystal, the ethylene diamine accepts the proton donated by *p*-phenol sulfonic acid furthermore the acceptor–donor strength [41] is significantly elevated owing to the intermolecular hydrogen bonding produced involving oxygen (negatively charged) atom in picrate anion with hydrogen of protonated nitrogen atom of piperazine.

#### 4.9. Antibacterial activity

Antibacterial proficiency of the EDDSM was measured using disc diffusion method [29]. The bacterial and fungal strains used for the

Table 5  
Antimicrobial activity of EDDSM.

Sl. no.	Bacteria/ Fungi	Zone of inhibition (mm in diameter)				
		20 $\mu$ L	40 $\mu$ L	60 $\mu$ L	80 $\mu$ L	Streptomycin/ Amphotericin B
1.	<i>Staphylococcus aureus</i>	13	15	18	20	30
2.	<i>Streptococcus</i>	13	15	15	20	18
3.	<i>Klebsiella pneumoniae</i>	13	13	13	16	23
4.	<i>Pseudomonas aeruginosa</i>	10	15	15	18	18
5.	<i>Aspergillus flavus</i>	13	9	13	16	30
6.	<i>Candida albicans</i>	15	15	15	18	30

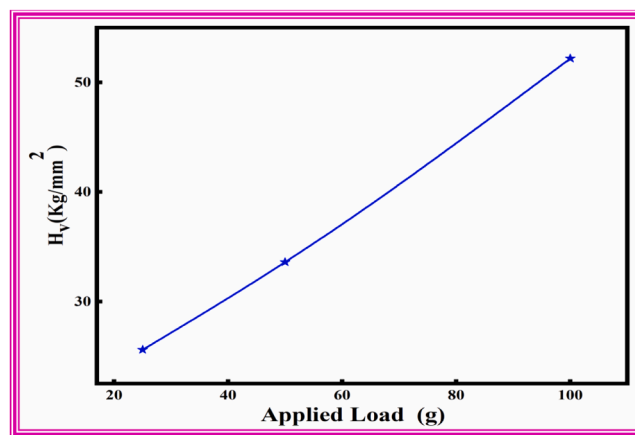


Fig. 11. Variation in microhardness number of EDDSM crystal with increase in load.

efficiency of the EDDSM such as *S. aureus*, *Streptococcus mutans*, *K. pneumoniae*, *P. aeruginosa* whereas *A. flavus* and *C. albicans* respectively. The activity of the synthesized compounds has been estimated by measuring the zone of inhibition in diameter against the tested microorganisms. Streptomycin was used as a positive control to compare the antibacterial screening results whereas Nystatin was used as a standard for antifungal studies. The antibacterial nature of the EDDSM was recognized against the tested pathogens and it was reported in Table 5.

The data revealed that the EDDSM exerting antagonistic activity in all the evaluated microorganisms. Especially, EDDSM exhibiting significant activity towards *Pseudomonas*, *Staphylococcus aureus* and *Streptococcus*. The mechanism behind the responses displayed permissible microbiological action in the cell walls of the bacteria. Further, the remaining investigated microorganisms also experiencing moderate antimicrobial activity. In the case of fungi, EDDSM demonstrates moderate antifungal activity against the evaluated fungal strains. EDDSM has shown potent antibacterial ability which reflects in the images with zone of inhibition as clearly indicated in Fig. 11. The results obtained from the disc images shows that the synthesized EDDSM possess good inhibitory action towards the selective microbes.

In addition, the activity of EDDSM against bacteria and fungi was displayed in terms of concentration and zone of inhibition as given in Fig. 12. The report inferred that the performance of EDDSM exhibiting remarkable changes in antibacterial and antifungal action as we compared to the standard. While increasing the concentration of EDDSM, the biological action of microbes was enhanced in *K. pneumoniae*, *Streptococcus* and *Staphylococcus aureus* which was illustrated graphically in Fig. 12.

Probably, the mechanism behind the antibacterial action towards the microorganisms emphasized that there is a possibility of EDDSM

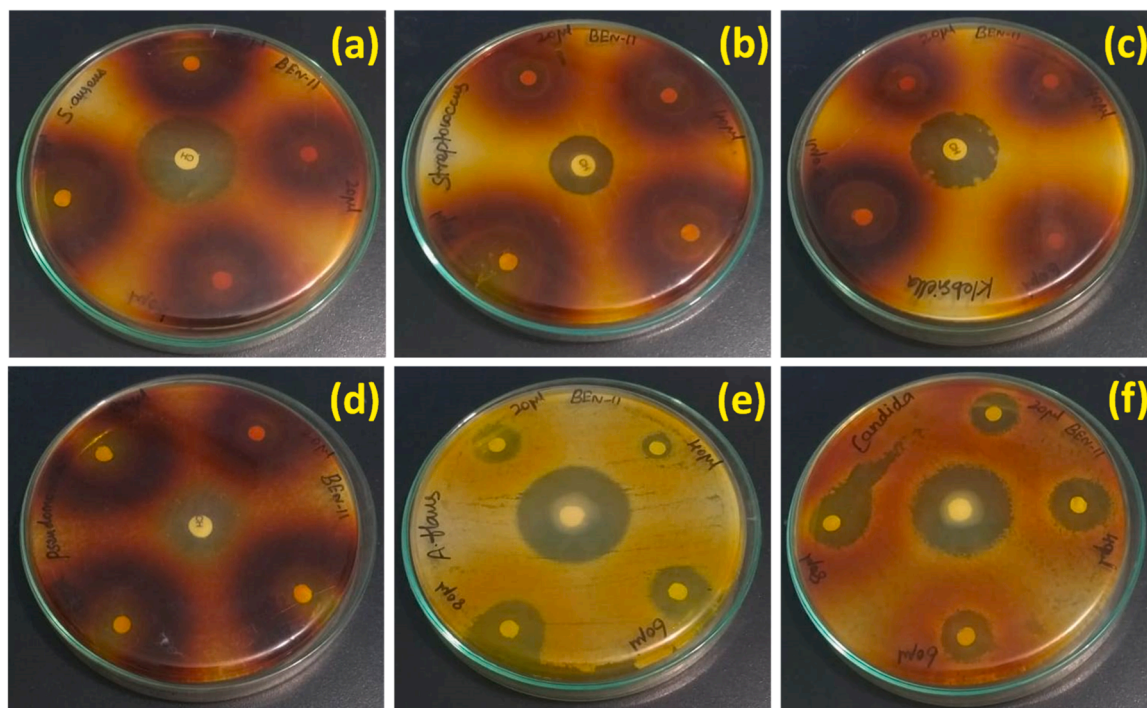


Fig. 12. Zone of inhibition of (a) *Staphylococcus aureus*, (b) *Streptococcus* (c) *Klebsiella pneumoniae*, (d) *Pseudomonas aeruginosa*, (e) *Aspergillus niger*, (f) *Candida albicans* with EDDSM.

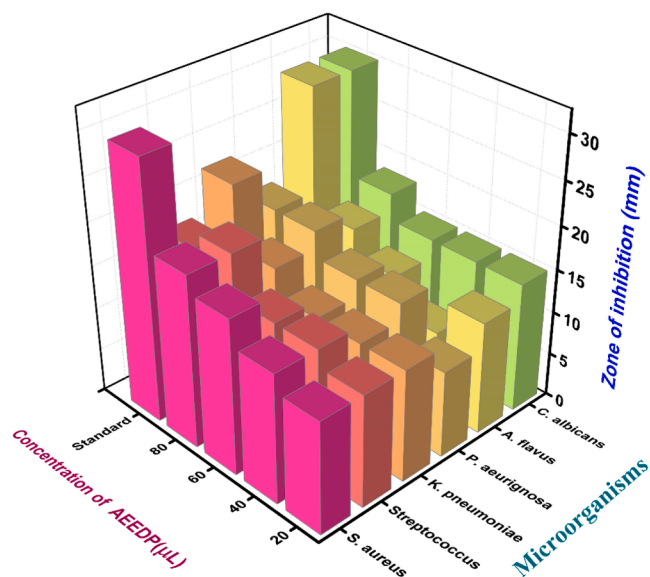


Fig. 13. The 3D histogram for the antimicrobial action of EDDSM with different concentrations in DMSO.

penetrates the bacterial cell wall which undergoes disruption thus leads to oxidative cell damage [42]. Hence, the above fact enhances the utilization of EDDSM in antimicrobial action (Fig. 13).

## 5. Conclusions

The 'bis-Ethylene Diammonium di-Phenolsulfonate monohydrate' (EDDSM) single crystal was amalgamated by slow evaporation solution technique with water and ethanol as blended solvents conducted at room temperature.

- The FTIR spectral studies establish that  $\text{CH}_2$  asymmetric vibrations corresponding to  $2488\text{ cm}^{-1}$  and  $2589\text{ cm}^{-1}$  exhibits highest percentage of transmittance. The smaller difference between these wavenumbers reveals that the reported crystal is much flexible and fast response.
- The EDDSM crystal exhibits cutoff wavelength is 299 nm with energy band gap of 4.17 eV. This shows that the crystal has an excellent transparency owing to the  $\pi-\pi^*$  transitions. Further, the Photoluminescence studies evidently disclose that the variation of intensity does not alter the position of emission peak with increase in excitation wavelength. The induced polarization does not influence optical emission of EDDSM crystal.
- Thermal studies reveal that EDDSM crystal exhibits thermal stability up to  $192\text{ }^\circ\text{C}$ . Further, the peak sharpness indicates the purity as well as crystalline nature of the composite.
- The comparative efficiency of EDDSM crystal with that of standard KDP sample was observed to be 1.2. The SHG for the EDDSM crystal is validated by a radiation of 532 nm. The grown crystal shows substantial evidence of NLO behavior although it belongs to centro symmetric group.
- The possible penetration of the EDDSM crystal into the bacterial cell wall causes disruption, which leads to the oxidative cell damage. Therefore, it justifies the antimicrobial action of EDDSM. This confirms that this organic single crystal has wide applications in industry and pharmacy.

## CRedit authorship contribution statement

**N. Rama Krishna Chand:** Writing – original draft, Validation, Investigation, Formal analysis, Conceptualization. **Y. Subba Reddy:** Validation, Formal analysis, Conceptualization. **J. Theodore:** Investigation, Formal analysis, Data curation. **M. Antilin Princela:** Writing – original draft, Methodology, Investigation, Formal analysis, Data curation. **S. Suguna:** Writing – original draft, Supervision, Project administration, Methodology, Investigation, Formal analysis. **P. Lakshmi Praveen:** .

## Declaration of competing interest

The authors declare that they have no conflict of interest.

## Data availability

All the Data included in the manuscript.

## Acknowledgment

The author N. Ramakrishna Chand and Y. Subbareddy acknowledges the support rendered by the FIST grant SR/FST/College-2017/48.

## References

- [1] J. Pecaut, Y. LeFur, R. Masse, *Acta Crystallogr. B* 49 (1993) 535.
- [2] P.N. Prasad, D.J. Williams, *Introduction to Nonlinear Optical Effects in Molecules and Polymers*, first ed., Wiley, New York, 1991.
- [3] R.W. Munn, C.N. Ironside, *Principles and Applications of Nonlinear Optical Materials*, Chapman & Hall, London, 1993.
- [4] S. Basu, A review of nonlinear optical organic materials, *Ind. Eng. Chem. Prod. Res. Dev.* 23 (1984) 183–186.
- [5] Y. Zhang, J. Li, B. Xi, Y. Che, J. Zheng, Growth and characterization of l-histidine nitrate single crystal, a promising semiorganic NLO material, *Mater. Chem. Phys.* 108 (2008) 192–195.
- [6] W. Denk, J.H. Strickler, W.W. Webb, Two-photon laser scanning fluorescence microscopy, *Science* 248 (1990) 73–76.
- [7] M. Rodriguez, G. Ramos-Ortiz, J.L. Maldonado, V.M. Herrera-Ambriz, O. Dominguez, R. Santillan, N. Farfan, K. Nakatani, Structural, thermal and optical characterization of a Schiff base as a new organic material for non-linear optical crystals and films with reversible noncentrosymmetry, *Spectrochim. Acta A* 79 (2011) 1757–1761.
- [8] B.R. Krishnamoorthy, S. Kannan, K. Sivaperuman, Synthesis and crystal growth of 2, 3-dimethyl-N-[2-(hydroxy) benzylidene] aniline: an organic second-order non-linear optical crystal for non-linear optical (NLO) applications, *Opt. Mater.* 113 (2021) 110864.
- [9] S. Muhammad, M. Nakano, A.G. Al-Sehemi, Y. Kitagawa, A. Irfan, A.R. Chaudhry, K. Fukuda, Role of a singlet diradical character in carbon nanomaterials: a novel hot spot for efficient nonlinear optical materials, *Nanoscale* 8 (42) (2016) 17998–18020.
- [10] S. Muhammad, H.-L. Xu, R.-L. Zhong, Z.-M. Su, A.G. Al-Sehemi, A. Irfan, Quantum chemical design of nonlinear optical materials by sp<sup>2</sup>-hybridized carbon nanomaterials: issues and opportunities, *J. Mater. Chem. C* 1 (35) (2013) 5439.
- [11] S. Muhammad, M. Nakano, Computational strategies for nonlinear optical properties of carbon nano-systems. Apple, No, Academic Press, New York, 2013, p. 24.
- [12] A. Anandhan, C. Sivasankari, M. Saravanabhavan, V. Siva, K. Senthil, Synthesis, crystal structure, spectroscopic investigations, physicochemical properties of third order NLO single crystal for optical applications, *J. Mol. Struct.* 1203 (2019) 127400.
- [13] G. Vadivelan, M. Saravanabhavan, V. Murugesan, M. Sekar, Synthesis, characterization and biological studies of a charge transfer complex: 2-aminopyridinium-4-methylbenzenesulfonate, *Spectrochim. Acta A* 145 (2015) 461e466.
- [14] M. Odabaşoğlu, O. Büyükgüngör, G. Turgut, A. Karadağ, E. Bulak, P. Lönnecke, Crystal structure, spectral and thermal properties of 2-aminopyridinium adipatemonoacidic acid dehydrate, *J. Mol. Struct.* 648 (2003) 133–138.
- [15] R. Chitra, R.R. Choudhury, T. Vijay, M.V. Hosur, G.T.N. Row, Molecular interactions in bis(2-aminopyridinium) malonate: a crystal isostructural to bis(2-aminopyridinium) maleate crystal, *J. Mol. Struct.* 1010 (2012) 46–51.
- [16] G. Sivaraj, N. Jayamani, V. Siva, Synthesis, structural, spectroscopic, mechanical, linear and nonlinear optical studies on 4-dimethylaminopyridinium p-toluenesulfonate: a comparative theoretical and experimental investigation, *J. Mol. Struct.* 1240 (2021) 130530.
- [17] K. Ramchandran, P. Vijayakumar, A. Raja, V. Mohankumar, G. Vinitha, M. Senthil Pandian, P. Ramasamy, Investigations of 4-methylbenzophenone (4MB) single crystal grown by Czochralski method and its characterization, *J. Mater. Sci.* 29 (2018) 8571–8583.
- [18] M.A. Bhat, A.A. Khan, H.A. Ghabbour, C.K. Quah, H.K. Fun, Synthesis, characterization, x-ray structure and antimicrobial activity of N-(4-chlorophenyl)-2-(pyridin-4-ylcarbonyl) hydrazinecarbothioamide, *Trop. J. Pharm. Res.* 15 (8) (2016) 1751–1757.
- [19] B.T. Rajeswari, P. Sathya, P. Dhanasekaran, G. Vinitha, S. Meyvel, V. Vijayalakshmi, J. Aarthi, First-time investigation on crystal growth, optical, thermal, electrical and third-order non-linear optical activities of novel thiosemicarbazide single crystals for non-linear optical applications, *J. Mater. Sci.* 32 (2021) 22984–22998.
- [20] S. Sagadevan, K. Pal, Z.Z. Chowdhury, et al., Structural, dielectric and optical investigation of chemically synthesized Ag-doped ZnO nanoparticles composites, *J. Sol-Gel Sci. Technol.* 83 (2017) 394–404.
- [21] T. Zaheer, S. Zia, K. Pal, et al., Recent trends in noble metals and carbon dots in the costume of hybrid nano architecture, *Top. Catal.* 67 (2024) 280–299.
- [22] A. Udayasri, M.M. Chandrasekar, M.V.B. Rao, G. Varanasi, D.S. Ramakrishna, Green chemical principles based regioselective functionalization of 2,4,6-trichloropyrimidine-5-carbaldehyde: application in the synthesis of new pyrimidines and pyrrolopyrimidine, *J. Serb. Chem. Soc.* 88 (2023) 1–9.
- [23] D.S. Ramakrishna, Preparation of novel chiral  $\alpha$ -diazocarbonyl compounds using Regitz's methodology, *Org. Preparations Proc.* Int. 54 (2022) 178–183.
- [24] G. Smith, U.D. Wermuth, Ethane-1,2-diaminium 4,4'-sulfonyl-dibenzolate, *Acta Crystallogr. E* 67 (2011) o2966.
- [25] P. Santharagavan, P. Ramasamy, *Crystal Growth Processes and Methods*, K.R.U. Publications, 1999.
- [26] M.N. Burnett, C.K. Johnson, ORTEP III. Report ORNL-6895, Oak Ridge.
- [27] G.M. Sheldrick, *Acta Crystallogr., Sect. A* 64 (2008) 122.
- [28] P. Jayaprakash, P. Krishnan, K. Suresh, K. Thillaivelavan, B. Dhinakaran, G. Vinitha, R. Ravisankar, Synthesis, growth and investigation of an efficient nonlinear optical single crystal: glycine potassium iodide, *Chem. Data Collect.* 34 (2021) 100752.
- [29] S. Suguna, Y. Subbareddy, T.J. Jose, N.R. Chand, D.S. Ramakrishna, P.L. Praveen, Synthesis, growth, and optical applications of N, N'-bis (2-aminophenyl) ethane-1,2-diammonium picrate: an organic crystal, *J. Mol. Struct.* 1300 (2024) 137295.
- [30] P. Kalsi, *Spectroscopy of Organic Compounds*, Wiley Eastern, New Delhi, 1985.
- [31] P.L. Praveen, *J. Mol. Liq.* 341 (2021) 117424.
- [32] T.J. Jose, A. Simi, et al., *Mol. Cryst. Liq. Cryst.* 665 (2018) 119.
- [33] M.M.C. Chou, L. Chang, C. Chen, W.F. Yang, *J. Cryst. Growth* 311 (2009) 448–451.
- [34] D.R. Hang, Mitch Chou, L. Chang, Y. Dikme, M. Heuken, *J. Cryst. Growth* 311 (2009) 452–455.
- [35] R. Kaliammal, G. Parvathy, R.M. Kumar, M.K. Kumar, G. Vinitha, S. Sudhakar, *Chinese J. Phys.* 72 (2021) 100–125.
- [36] K.E. Rieckhoff, W.L. Peticola, *Science* 147 (1965) 610–611.
- [37] V.V. Ghazaryan, M. Fleck, A.M. Petrosyan, *Spectrochim. Acta A* 78 (2011) 128.
- [38] M. Shakir, S.K. Kushwaha, K.K. Maurya, M. Arora, G. Bhagavannarayana, *J. Cryst. Growth* 311 (2009) 3871–3873.
- [39] T. Dhanabal, M. Sethuraman, G. Amirthaganesan, S.K. Das, *J. Mol. Struct.* 1045 (2013) 112–123.
- [40] S. Suguna, J.V. Jovita, D. Jeyaraman, K.S. Nagaraja, B. Jeyaraj, *Int. J. Chem. Tech. Res.* 8 (2015) 249–259.
- [41] D.S. Ramakrishna, T.J. Jose, P.L. Praveen, *J. Mol. Struct.* 1236 (2021) 130336.
- [42] C.I. Sobanaraj, M.A. Príncipe, Efficiency of Salen functionalized ionic liquids and their application towards biological activity, *Int. J. Pharm. Sci. Nanotechnol.* 13 (2020) 5020–5027.